
Modelling mine gas explosive pattern in underground mine gob and overlying strata

Jianwei Cheng*

State Key Laboratory of Coal Resources and Safe Mining,
University of Mining and Technology,
Xuzhou, Jiangsu, 221116, China
and
Key Laboratory of Gas and Fire Control for Coal Mines,
College of Safety Engineering,
China University of Mining and Technology,
Xuzhou, Jiangsu, 221116, China
Email: Cheng.Jianwei@cumt.edu.cn
*Corresponding author

Chang Qi and Siyuan Li

Key Laboratory of Gas and Fire Control for Coal Mines,
College of Safety Engineering,
China University of Mining and Technology,
Xuzhou, Jiangsu, 221116, China
Email: ts17120011a3@cumt.edu.cn
Email: lsy@cumt.edu.cn

Abstract: A 3D physical experimental model is well designed to simulate a U-type underground mine working face. Based on two important influence factors, the air quantity delivered into the ventilation system and the gas release rate (GRR) in gob, a series of experiments are designed to examine the range pattern of gas explosive zone changing in the mine gob with following various combinations of air velocities and GRRs. By sampling works, the gas concentration could be obtained at different horizontal levels and vertical lines in the experiment model. The experimental results show various shapes and areas of explosive zones in gob and in overlying caved spaces as the GRR and air velocities change. This research work is of great reference for mining engineers to apply the ventilation design practices to minimise the explosion hazard risk in a mine gob area. [Received: July 26, 2017; Accepted: December 13, 2017]

Keywords: modelling; mine gas; explosion; explosive pattern; 3D physical experimental model; physical simulation; gas release rate; GRR; air quantity; underground ventilation; mine gob; rock strata similarity; ventilation flow field similarity; gas distribution; overlying strata; coal.

Reference to this paper should be made as follows: Cheng, J., Qi, C. and Li, S. (2019) 'Modelling mine gas explosive pattern in underground mine gob and overlying strata', *Int. J. Oil, Gas and Coal Technology*, Vol. 22, No. 4, pp.554–577.

Biographical notes: Jianwei Cheng is an Associate Professor at the China University of Mining and Technology and Australia 'endeavour' Research Fellow at the Curtin University. He graduated from the West Virginia University (USA) with PhD degree. He is now teaching and researching in the field of underground mining safety.

Chang Qi is currently studying for his Master degree at the China University of Mining and Technology. Currently, he is doing research on explosion protection problems in the industrial safety.

Siyuan Li is currently studying for his Master degree at the China University of Mining and Technology. Currently, he is doing research on explosion protection problems in the industrial safety.

1 Introduction

The underground coal mine gas, which is composed of either biogenically or thermogenically-derived gas during the process of coal formation. Flores (1998) state is an unconventional gas resource and is adsorbed into the coal seam reservoir. With the mechanised mining technology applied, a considerable exposure area of the gassy coal seam, surrounding rock and residual coal pieces appear, in which the in-seam gas pressure drops below the critical limit of desorption pressure. Thus, a great amount of free mine gas, especially from the coal seam and residual coal pieces, would emit into mining spaces. Because of the potential coal spontaneous combustion in gob and its inaccessibility, once a flame appears in gob, it is difficult to be extinguished within a short period of time. It may trigger an explosion in gob which then expands to other parts of underground mine.

In China, there are five major hazardous sources in underground coal mine, among which the gas explosion is considered to be the most serious one and has caused many fatalities and huge property losses over the past few decades. During 2001–2010, gas explosions caused a total of 675 coal mine accidents and 6,075 deaths, which accounted for 35.53% of the total of 1,900 all accidents and 44.97% of fatalities respectively (Chen et al., 2012). In addition, gas from the adjacent coal seam could migrate into the gob through the fractures in surrounding strata. A caved zone behind the working face, which is highly fragmented, generally extends upwards three to six times of the mined-out coal seam thickness (Singh and Kendorski, 1981; Palchik, 2003). The methane stored in the caved zone would also be released during the mining process, which is a large coal gas contributor to the gas volumetric concentration in underground mine ventilation system (Dougherty et al., 2010). Once the coal is extracted, both the ground pressures of the overlying and underlying coal strata are released and the fractures are extensively created in rocks and strata, which give pathways for the gas migrating to mine gob space and the gas concentration could build up (Choi et al., 1997; Karacan et al., 2011; Wang et al., 2015; Schatzel et al., 2012). Meanwhile, Airey (1968) studies that the coal gas also emits from the residual coal pieces left in gob which plays another contributor to increase the gas concentration. Thus, the gob, actually, is a major mine gas storage site in an underground coal mine. Furthermore, due to the atmospheric pressure differences in various underground locations, the gob mine gas could flow into the underground working

sections by the ventilation system, which also induce the gas concentration increasing in miners' workplaces and threatens the safety of miners. The mine gas migration and emission from the gob are strictly controlled by the geology, mining methods and gas content in coal seams (Diamond et al., 1994; Balusu et al., 2001).

Statistics shows a large number of gas explosion accidents occurred at the upper corner of working face and the mine gob where methane concentration could easily build up to reach the explosive limit. For purposes of mine gas prevention and control, the study of methane migration and distribution pattern in a mine gob has been attracted by many mining researchers (Hu et al., 2009, 2008). It has been advised that an underground working faces would be insured safely once the 80%–94% of total mine gas in coal seams is removed (Curl, 1978; Schatzel et al., 1992). One effective way is to minimise methane emission into working places by using the gob gas venthole (GGV) (Karacan, 2015; Liu et al., 2016) to drain the coal gas. A basic strategy of gas control in underground is to increase the ventilation airflow for sweeping the longwall working face and diluting the gas concentration (Cheng et al., 2016). However, this also results in a quantity of fresh air leaking into the mine gob area, which may greatly change the gas concentration pattern (Mishra et al., 2016; Torano et al., 2009). As the overlying strata collapse behind the longwall working face, the underground mine gob area is filled with fractured rocks with the toxic gases accumulating, which makes the gob to be an extremely dangerous and inaccessible zone (Stoltz et al., 2006; Prosser and Oswald, 2006). It is impossible for researchers to perform any direct measurements of gas concentration in an actual gob to really characterise the distribution pattern. Therefore, not many researches have been comprehensively performed on this problem. Therefore, to better study the migration and concentration distribution of coal gas, it is necessary to make a scaled physical model of mine gob which catches the main features of the real situation (Lunazewski, 1998; Karacan et al., 2007) to model the gas concentration distribution in both gob area and deformed overlying strata under various conditions.

In this research, a physical mine gob model with several overlying strata is built, which can fully simulate the development of a gob formation due to the overlying strata caving when the coal is mined out. In addition, the gas is sampled from each measuring points at different levels through the pre-set the measurement tubes and the corresponding explosion analyses are done to help figure out the gas distribution and explosive zones in the mine gob. The results are of great reference for mining engineers to understand the ventilation patterns and explosion hazard in mine gob.

2 Background of mine gob and longwall working face

The designed physical model is based on a gassy coal mine, the Datong #1 mine located in Chongqing, China. The width of longwall panel of the mine is 210 m and the average overlying strata depth is 70 m. A mining height of 3 m is used. Table 1 shows the lithology column and Table 2 shows mechanical properties of each stratum.

According to the ventilation records obtained from the mine as shown in Table 3, the air velocities in intake and return roadways are 1.24–2.61 m/s and 1.82–3.98 m/s, respectively. The exhaust system is applied as the ventilation system. According to the most recent records, the GRR fluctuated with the time from 25.41 m³/min to 60.86 m³/min, which could be instructive for setting a reasonable simulated GRR in experiments.

Table 1 Geological columnar over the longwall panel (see online version for colours)

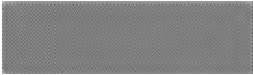

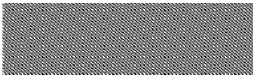

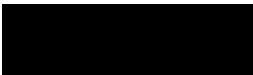







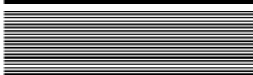
<i>Depth (m)</i>	<i>Thickness (m)</i>	<i>GeologyColumnar</i>	<i>Lithology</i>
1	1		Top soil layer
8	7		Packstone
11	3		Siltstone
14	2		Mudstone/siltstone
15	1		Jurassic coal seam
23	9		Sandstone
32	9		Glutenite/sandstone
49	17		Mudstone/sandstone
56	7		Sandstone
61	5		Sandstone
64	3		Lamprophyre
66	3		Current mining coal seam
70	2		Sandstone

Table 2 Mechanical properties of overburden strata

<i>Layer name</i>	<i>Density (kg/m³)</i>	<i>Elasticity modulus (MPa)</i>	<i>Poisson ratio</i>	<i>Cohesion (MPa)</i>	<i>Frictional angle (°)</i>	<i>Strength (MPa)</i>
Top soil layer	1,854	11	0.34	0.02	17	0.72
Packstone	2,730	2,357	0.22	3.43	28	35.54
Siltstone	2,554	1,575	0.21	2.84	31	82.92
Mudstone/siltstone	2,740	2,310	0.22	3.33	28	45.84
Coal seam	1,329	1,355	0.34	1.18	24	30.90
Sandstone	2,755	2,205	0.24	3.33	28	77.25
Glutenite/sandstone	2,611	1,680	0.22	2.45	31	98.47
Mudstone/sandstone	2,730	2,357	0.22	3.43	28	45.32
Sandstone	2,750	1,906	0.26	3.58	28	77.25
Sandstone	2,755	2,205	0.24	2.45	28	77.25
Lamprophyre	2,760	3,150	0.18	3.33	29	44.08
Coal seam (current mining)	1,329	1,355	0.34	1.18	24	16.48
Sandstone	2,750	4,257	0.19	3.92	31	92.70

Table 3 Field data of ventilation and methane drainage in Datong 1# coal mine

No.	Date	CH4 concentration/%	Air velocity/ m/s		Methane drainage quantity/m ³ /min
			Intake	Return	
1	January 1, 2015	1.2	1.24	1.82	27.9
2	February 1, 2015	3.34	1.77	2.87	35.63
3	March 1, 2015	2.64	1.92	3.10	37.81
4	April 1, 2015	3.16	1.91	3.09	39.81
5	May 1, 2015	3.25	1.91	3.09	25.41
6	June 1, 2015	2.98	1.78	2.88	47.55
7	July 1, 2015	3.37	1.85	3.21	45.62
8	August 1, 2015	2.73	1.83	2.96	53.53
9	September 1, 2015	2.86	2.15	3.98	53.15
10	October 1, 2015	3.03	2.09	3.38	36.53
11	November 1, 2015	3.24	2.09	3.38	60.86
12	December 1, 2015	3.41	1.96	3.18	48.05
13	January 1, 2016	3.26	1.55	2.51	37.9
14	February 1, 2016	3.26	1.58	2.56	45.63
15	March 1, 2016	3.20	1.66	2.69	47.81
16	April 1, 2016	1.64	1.45	2.35	49.81
17	May 1, 2016	1.86	1.58	2.55	35.41
18	June 1, 2016	1.5	2.61	3.08	47.55

Figure 1 shows the geological column of the overburden strata. A total of nine measuring levels are set in the overlying strata.

Figure 1 Coal seam overlying strata and measuring levels arrangement (see online version for colours)

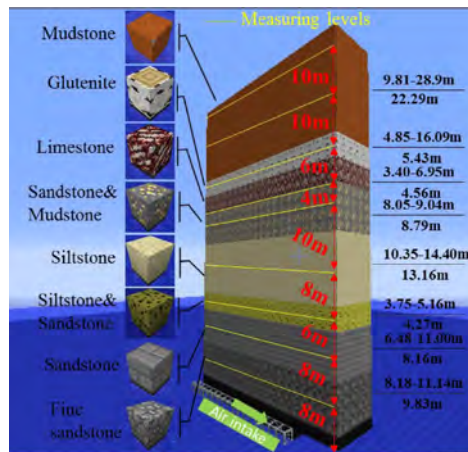


Table 4 Materials used in physical modelling

<i>Strata</i>	<i>Thickness (mm)</i>	<i>Total material quality (Kg)</i>	<i>Component ratio (S:L:G)</i>	<i>Sand quality (Kg)</i>	<i>Lime quality (Kg)</i>	<i>Gyp sum quality (Kg)</i>	<i>Water quality (Kg)</i>
Top soil layer	1	118.50	11:01:00	108.6	9.88	0.00	11.85
Packstone	7	133.80	11:08:02	70.09	50.97	12.74	13.38
Siltstone	3	120.90	9:06:04	57.27	38.18	25.45	12.09
Mudstone/siltstone	2	120.00	9:08:02	56.84	50.53	12.63	12.00
Jurassic coal seam	1	122.10	8:09:01	54.27	61.05	6.78	12.21
Sandstone	9	143.70	7:06:04	59.17	50.72	33.81	14.37
Glutenite/sandstone	9	141.60	5:05:05	47.20	47.20	47.20	14.16
Mudstone/sandstone	17	143.70	10:09:01	71.85	64.67	7.19	14.37
Sandstone	7	99.90	9:07:03	47.32	36.81	15.77	9.99
Sandstone	5	93.60	9:06:04	44.34	29.56	19.71	9.36
Lamprophyre	3	96.30	10:08:02	48.15	38.52	9.63	9.63
Permian coal seam (current mining)	3	114.90	9:06:04	54.43	36.28	24.19	11.49
Sandstone	3	161.70	7:04:06	66.58	38.05	57.07	16.17

3 Simulation experiment

3.1 Physical model frame and similarity ratios

3.1.1 Rock strata similarity

In building such physical model, a dimension scale (e.g., the scale of real depth and model depth) should be determined firstly. Based on the dimension scale, the other scales for force, velocity, strain, stress (strength) can also be determined. These scales are the bases for determining the required mechanical properties of the simulating rock layers and ventilation flow characterises for interpreting the simulation results.

The mentioned working face and overlying strata are scaled down to a 3D multi-strata physical model. The dimension of the model is designed as 3,000 mm × 2,100 mm × 700 mm (length, width and height). Thus, the geometric similarity ratio is:

$$C_l = \frac{210 \text{ m}}{2100 \text{ mm}} = 100 \quad (1)$$

Which means the thickness of the coal seam in the model is 32 mm representing the 3.2 m thickness of the coal seam.

According to the similarity principles, the physical model must be similar to the prototype underground coal mine working face geometrically, kinematically and dynamically. The working face and overlying strata agree with the actual working face layout and strata properties. In the same way, according to the properties of selected simulation materials, the constant bulk density ratio can be calculated as 1:1.6 which represents the specific gravity of the stratum in the prototype vs. the specific gravity of this stratum in the model. It is also possible to determine the actual deformation of overlying using such ratios, the time ratio should be 1:10. The mining speed in the model is 21 mm/h which represents the mining advance rate of 12 m/d in the prototype system.

The materials for physical model are combinations of gypsum, concrete, sand and lime. The grain size of the sand is within 0.15–0.5 mm. The lime is made from freshwater limestone and through-burned. The gypsum is calcined. Mica is used to imitate the bedding planes. Different types of strata can be simulated by changing the weight ratio of sand, lime and gypsum (S:L:G). The key mechanical parameters of simulated strata are shown in Table 4.

3.1.2 Ventilation flow field similarity

One principle factor of flow similarity among two fluids is that their flow condition satisfies geometric similarity, kinematics similarity and dynamic similarity. In the previous sections, the geometric similarity has been discussed and applied to design the physical model. Kinematics similarity requires that the length and time scales are similar between model and prototype. Obviously, kinematics similarity includes geometrical similarity (Jones, 1969; Kundu and Cohen, 2008). Dynamic similarity exists between geometrically and kinematically similar systems, and it requires that the ratios of all forces acting on corresponding fluid particles and boundary surfaces in the model and prototype are constant (Konduri et al., 1997). In fact, model and prototype flow cannot become equal flow and fully dynamic similarity (Wallerstein et al., 2002); therefore, the main dynamic similarity is a key point of the simulation experiments. For the steady flow

of the incompressible fluid, the Reynolds number of two different flow types must be similar, which can be expressed as:

$$(\text{Re})_m = (\text{Re})_p; \frac{V_m l_m}{\nu_m} = \frac{V_p l_p}{\nu_p} \quad (2)$$

where m is the model, and p is the prototype. V is the average velocity in the roadway, m/s; ν is the dynamic viscosity coefficient of the fluid, related to fluid temperature and pressure and l is the characteristic linear dimension, m . Thus, they have dynamic similarity.

In order to meet this similarity criterion, the flows in the model and prototype must be similar. The hydraulic diameter of underground prototype roadways is 4.5 m. Thus, it is design that a diameter of 450 mm tube is placed on two sides of the model to simulate the underground roadways. The geometric similarity ratio is chosen as:

$$w_l = \frac{4.5 \text{ m}}{450 \text{ mm}} = 10 \quad (3)$$

In the experiment, the fresh air is also used. Thus, following the equation (2), the velocity in intake and return roadways of prototype ranges from 1 m/s to 4 m/s would be scaled from 10 m/s to 40 m/s.

3.2 Model description

A photo of experimental model and a design blue print are shown in Figure 2. Two PVC tubes are placed on both sides to form a U-type ventilation system, and a gas release channel is set on the right side. As shown within yellow frame, the lower part of the physical model, which looks like a container is composed of a steel frame surrounded by eight steel plates. In order to show the strata deformation clearly, the two front plates are replaced with glass ones later.

Figure 2 Physical model and design (see online version for colours)

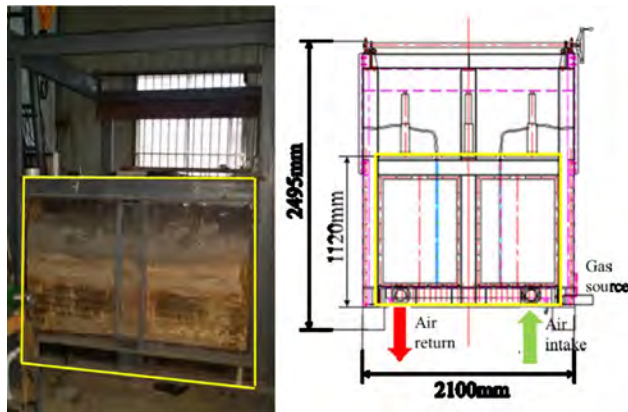
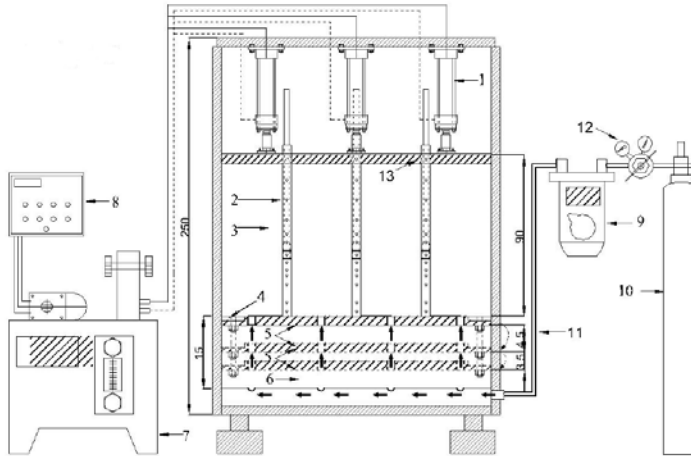


Figure 3 Detail introductions to physical model



Notes: 1 – hydraulic cylinder, 2 – intake pipe, 3 – test area, 4 – immovable steel plate, 5 – lifting steel bar, 6 – air chamber, 7 – hydraulic pump, 8 – distribution box, 9 – flow metre; 10 – gas bottle, 11 – hose, 12 – pressure reducing valve, 13 – pressure plate.

Figure 4 Sampling system and pumping tube design (see online version for colours)



The strata seams are simulated by means of different combinations of limestone, sands and calcium carbonate mixed with water. Hence, the strength of prototype rocks could be well represented. When the ‘mining process’ is initiated, the lifting steel bar could move to extract the coal seam, and the hydraulic cylinder is used to simulate the ground pressure to exert a loading pressure (the ground pressure) coming from strata seams over such simulated ones. Thus, the strata deformation occurs and the bottom strata would even collapse to a great amount of porous media which would fill the gob area. This process well presents the characteristics of a real gob. Then, the whole model is perfectly sealed. A special gas sampling and measuring system is built to take the gas samples at the two levels within the gob and the other nine levels in overlying strata. Figure 4 shows the matrix of pre-set tubes drilled with holes at different levels. A gas sampling chamber

can be pulled upward or pushed downward to a certain height where a hole has been punched through the tube wall. Then, the gas samples for the concentration analysis can be taken with a negative sampling device. By repeating sampling and measurement procedures, the gas concentration in the gob and overlying strata could be obtained.

In addition, two levels that are close to gob roof and floor respectively are set in the gob separately, which are not shown in Figures 2 and 3 but partially zoomed in Figure 5 (named as level 1 and 2). The layout of 12 measuring points at each measuring level above the gob is the same as that at level 1 and 2 shown in Figure 5.

Figure 5 Measuring level and points in physical model (see online version for colours)

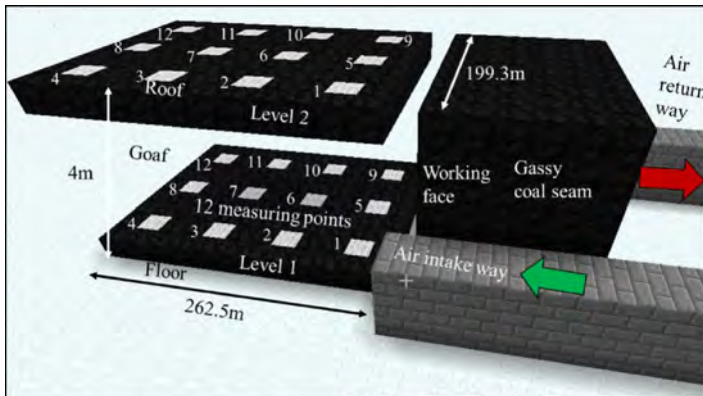


Figure 6 Negative sampling pumper devices and methane concentration diameter (see online version for colours)



To obtain more detailed information about the gas distribution in a mine gob and upper caved strata space, two levels are set within the gob and nine levels are set in overlying strata. At each level, a matrix of 12 measuring points is arranged to make the gas concentration measurement more specific. Figure 6 presents the sampling and measuring

instruments used in the experiment: on the left is a negative-pressure pumper and on the right is gas volumetrical concentration detector.

Figure 7 Axial flow fans used (see online version for colours)



Figure 8 Wind velocity anemometer (see online version for colours)



Figure 9 Gas rotor flow metre (see online version for colours)



Before starting the sampling and measuring work, the two axial fans providing air circulation (as shown in Figure 7) are used to simulate the underground ventilation system. Figure 8 presents the velocity anemometer used to control the air velocity in PVC tubes (simulated as ‘intake’ and ‘return’ roadway). The valve of gas source is then turned on and the gas release is controlled by a flow metre shown in Figure 9. As the equipment runs for a while, the gas fills the gob up and the ventilation pattern becomes relatively stabilised. Then the sampling work can begin. The gas sampling chamber can be pulled to different levels to take the gas samples. Once gas samples and gas concentration distribution are obtained under a preset testing combination of GRR and air velocities, the above-described operation is to be repeated for other combinations.

4 Experimental plans

To develop relatively stable gas concentration distribution patterns which are meaningful under pre-set similarity ratio modelling, it is necessary to note that the ventilation condition or gas release in the gob area is always changing with the time, which could be verified by the records in Table 3. Meanwhile, the combination of air velocities and GRRs varies in any given time. Hence, considering the representativeness of the combination of two parameters and the similarity principles, four different GRRs are set in the experiment: 0.17 m³/min, 0.33 m³/min, 0.50 m³/min, 0.67 m³/min in model, which correspond respectively to 16.67 m³/min, 33.33 m³/min, 50 m³/min, 66.67 m³/min in real mine situation (as shown in Table 5). Besides, three modes of combination of air velocities in air intake way and return way, in accordance with the field testing of air velocity, are proposed, which are shown in Table 6. The gas concentration data collection can be done under such 12 different combination cases.

Table 5 Various GRRs in experiment

<i>GRRs (m³/min) in model</i>	<i>GRRs (m³/min) in prototype</i>
0.17	16.67
0.33	33.33
0.50	50
0.67	66.77

Table 6 Types of combination of air quantities in air intake way and air return way

<i>Air quantities combination mode (CM)</i>	<i>Air velocity (m/s) in model</i>		<i>Air velocity (m/s) in prototype</i>	
	<i>Intake roadway</i>	<i>Return roadway</i>	<i>Intake tube</i>	<i>Return tube</i>
CM 1	10	20	1	2
CM 2	20	40	2	4
CM 3	25	35	2.5	3.5

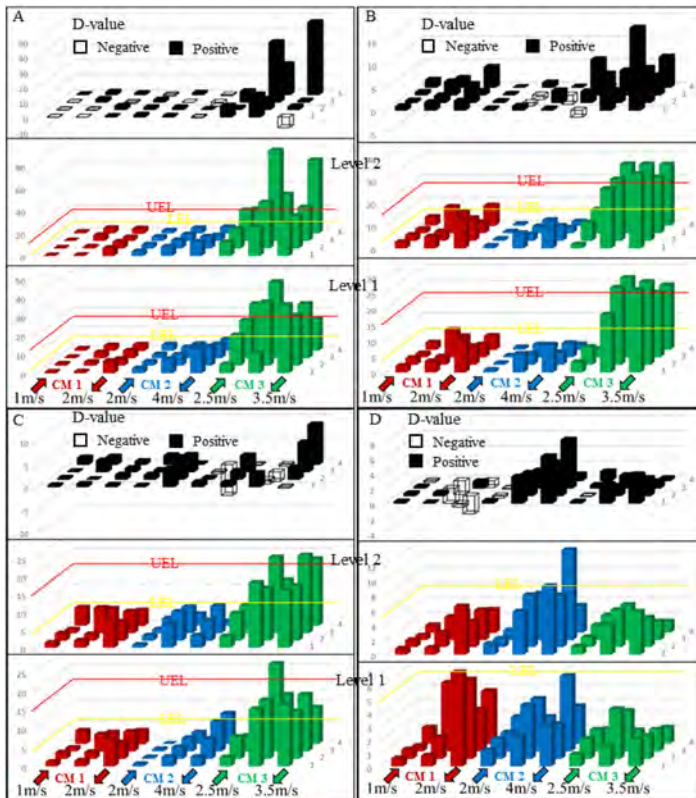
As a result, a total of 12 groups of data can be taken from 12 × 11 sampling points from the model gob and overlying strata under the combinations of four different GRRs and three modes of ventilation air quantities.

5 Results and discussions

5.1 Gas distribution within the gob

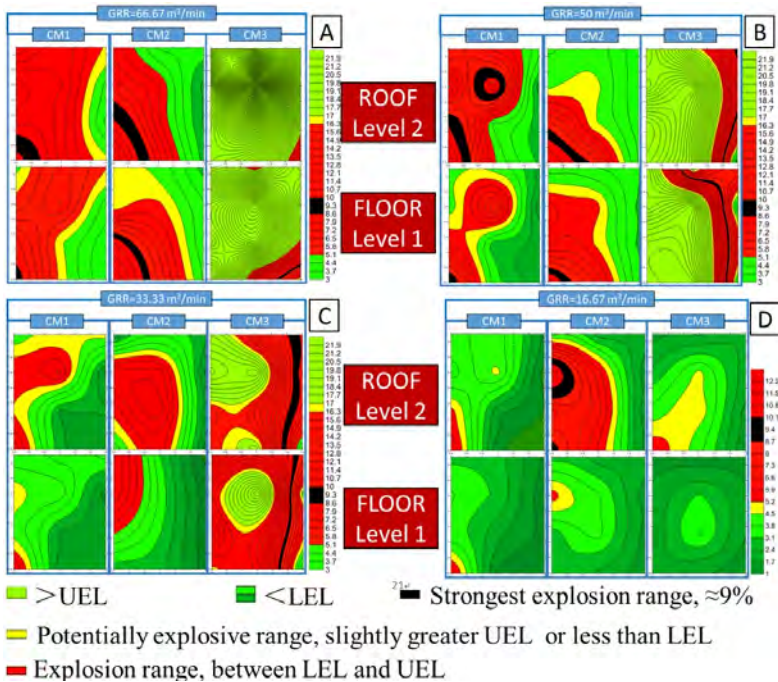
As mentioned before, the gas concentration on the 11 levels (two in the gob and nine in the overlying strata) can be obtained under 12 ventilation patterns (combinations of four GRRs and three modes of air velocity in intake and return way). Figure 10 represents a comprehensive summary of all the data obtained in the experiment with a column chart. It shows how gas distributes in the gob under a certain pattern. The lower two colourful figures (in A, B, C and D) present the gas concentration data from two levels of roof and floor, with the black/white columns showing the difference value (D-value) between these two levels. As an example, when the concentration at a measurement point on level 2 (roof level) is greater than the lower corresponding one on level 1 (floor level), D-value is positive and represented by a black solid column in the black/white column chart at the same point and vice versa.

Figure 10 Gas concentration distribution chart (see online version for colours)



As is shown in Figure 10, there are four groups of data, namely A, B, C and D in different conditions of GRR at 16.67 m³/min, 33.33 m³/min, 50 m³/min, 66.67 m³/min, respectively. The colours (red, blue and green) of columns present different air velocities in intake and return roadways as for CM 1, 2 and 3. It also can be seen that the gas concentration on different levels is varied with a general trend that the gas concentrations on level 2 are greater than those on level 1. For example, in case of CM 3, the D-values are positive and huge; and the gas concentration is significantly greater than that of the other two air velocity combinations. However, a noteworthy exception is that the red and blue columns are apparently higher than the green one when GRR is 16.67 m³/min. This indicates that, in most GRR cases (16.67 m³/min, 33.33 m³/min, 50 m³/min), the combination CM 3 could make a higher gas concentration compared with the other two combinations, which means more gas emission from the gob and more explosion risks. In other words, once the GRR is set at 16.67 m³/min, 33.33 m³/min, 50 m³/min, either CM 1 or CM 2 is suitable for gas control purpose. In contrast, when GRR is large enough (66.67 m³/min), CM 3 could hold most of gas within the gob area, only a small part of gas escaping to working faces. Thus it is more helpful to mitigate the explosion risk compared with the other two CMs.

Figure 11 Contour map of methane concentration on different levels in the gob (see online version for colours)



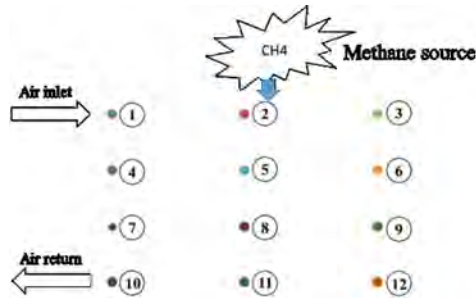
The gas concentration contour map in the gob on two levels with a height of 0 m and 4 m (close to floor and roof respectively) under different GRRs are shown in Figure 11 (A, B, C and D representing the same items as in Figure 10). To visibly present the explosion risk on two levels, five colours are employed in different areas indicating the likelihood of gas explosion. The black zone is the most explosively hazardous area in the gob because the gas concentration at these zones is very close to 9% which amounts to the strongest explosion intensity concentration for methane. The red represents the explosion range. The light yellow strip-type zones represent the areas at which methane concentration are very close to upper explosive limit (UEL) or lower explosive limit (LEL). The areas shaded in green and light green represent the gas concentration either over UEL or below LEL. The concentration could fall in the gas explosion range at any time due to the fluctuation of ventilation and gas release rate (GRR).

The general patterns of gas concentration on the gob floor and gob roof are shown in Figure 11. As indicated, the space close to the gob roof has more explosion risks with a larger explosive/potential explosive area, which could also be seen from Figure 10. In Figure 10, the D-value of two adjacent curves is unified (0.7%). This means the concentration is greater as the corresponding zones of curves are thicker, and vice versa. The gas concentration distribution in the gob area is greatly influenced by the ventilation and gas release from the residual coal pieces and rock in the gob area, which makes it necessary to understand the integrative effect of ventilation and gas release on gas distribution in underground mines so as to choose a suitable ventilation plan. Sometime, simply increasing air quantities in both air intake way and return way may not be helpful for gas control. For example, the left two figures of CM 1 in Figure 11(c) is more effective for gas control than increasing both air velocities to CM 3. Through analysing Figure 11, it can be drawn that CM 1 is the best ventilation strategy for gas control when the GRR is 16.67 m³/min or 33.33 m³/min, while CM 2 is suitable when the GRR reaches 50 m³/min. CM 3 should be adopted when GRR is 66.67 m³/min, because contrary to diluting the gas in the gob by ventilation, these air quantities just keep the gas in the gob at a very high concentration which makes an explosion impossible to occur. What is worth reminding is that CM 1 is not suitable for gas control when GRR are 50 m³/min and 66.67 m³/min, because it diffuses the gob gas and enlarges the explosive area; similarly, setting ventilation as CM 3 is not a good choice when GRR is 33.33 m³/min.

5.2 Gas distribution within overlying strata

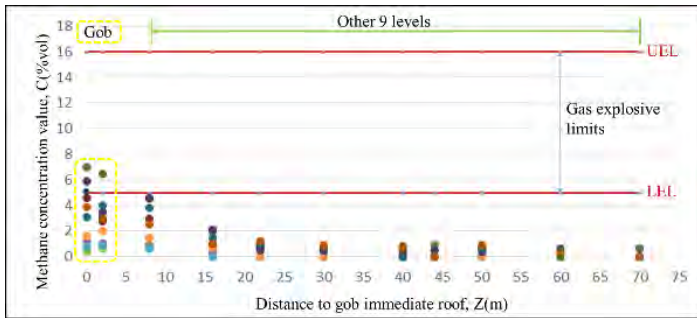
In order to study the comprehensive influence of air quantities and GRR on gas distribution patterns in overlying caved space, nine of 11 measuring levels are set into the strata over gob roof. Figure 12 shows the basic layout of ventilation system, gas source and numbered measuring points. Figure 13 to 15 present the scattering diagrams of gas concentration under different combinations of CM 1, CM 2, CM 3 and four GRRs. In other words, the gas concentration pattern in both the gob and the overburden is studied with the GRR changing under CM 1, CM 2 and CM 3. All 11 measuring levels are distributed along the X-axis according to their heights over the gob floor, and the scattering points in yellow dotted frame are gas concentration data from two measuring levels in the gob which have been analysed in details above (Figure 10).

Figure 12 Schematic diagram of arrangement of ventilation, methane source and measuring points' numbering (see online version for colours)

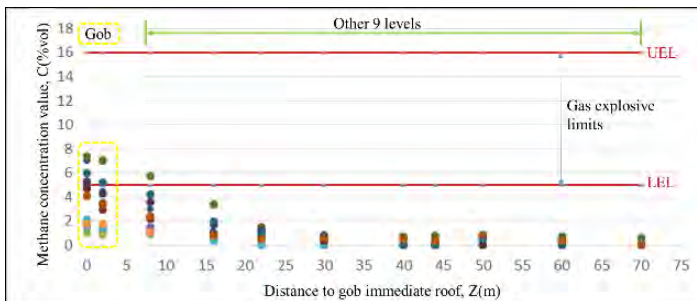


From Figures 13 to 15, it can be noted that:

Figure 13 Scattering diagram of methane concentration values under different methane releasing rate when air quantities in air intake way and return way are separately 1m/s and 2m/s (CM 1), (a) GRR = 16.67 m³/min (b) GRR = 33.33 m³/min (c) GRR = 50 m³/min (d) GRR, = 66.67 m³/min (see online version for colours)

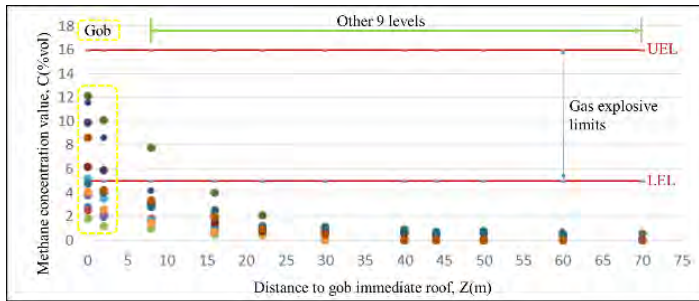


(a)

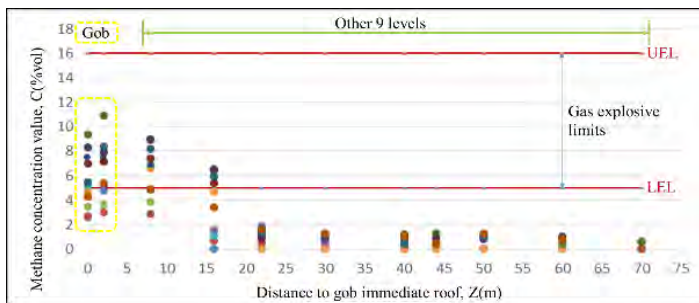


(b)

Figure 13 Scattering diagram of methane concentration values under different methane releasing rate when air quantities in air intake way and return way are separately 1m/s and 2m/s (CM 1), (a) GRR = 16.67 m³/min (b) GRR = 33.33 m³/min (c) GRR = 50 m³/min (d) GRR, = 66.67 m³/min (continued) (see online version for colours)



(c)

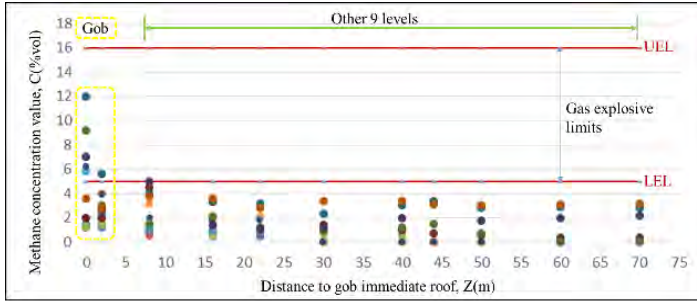


(d)

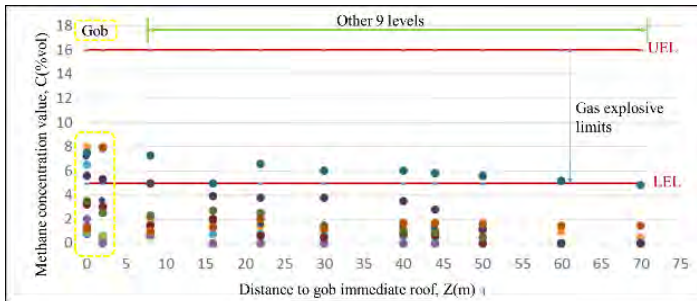
As shown in Figure 13, under the ventilation condition of CM 1, more and more gas explosive zone arises in the gob area with GRR increasing, while the gas concentration in levels above 30 m remains low and stable. An enlightening phenomenon is that when GRR is set at 50 m³/min, some part (8.3%) of measuring level, about 8 m above the gob floor in overlying strata, is explosively hazardous.

From Figure 14, it can be seen that when both air quantities in air intake/return way are doubled compared with in the above case, and GRR is set as 33.33 m³/min, point no. 11 close to the air return way on all levels is explosive because the gas data measured there are between LEL and UEL. From Figure 13(d), it can be concluded that under this GRR and CM 2, the overlying strata (8–22 m off the gob floor) contain explosive zones of various sizes, because the gas concentration data concentrate between the limits of gas explosion.

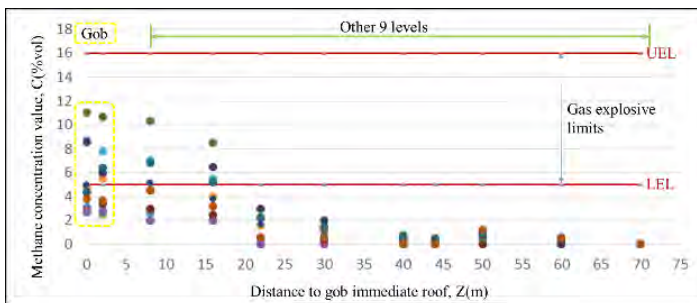
Figure 14 Scattering diagram of methane concentration values under different methane releasing rate when air quantities in air intake way and return way are separately 2 m/s and 4 m/s (CM 2), (a) GRR = 16.67 m³/min (b) GRR = 33.33 m³/min (c) GRR = 50 m³/min (d) GRR = 66.67 m³/min (see online version for colours)



(a)

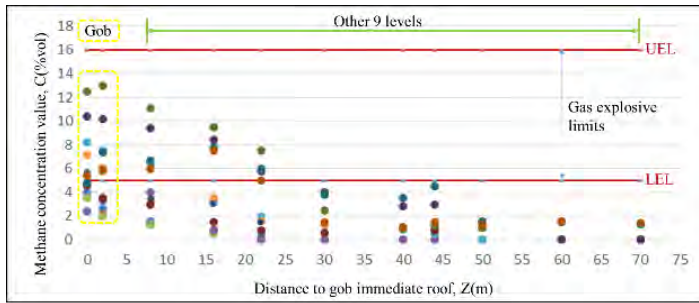


(b)



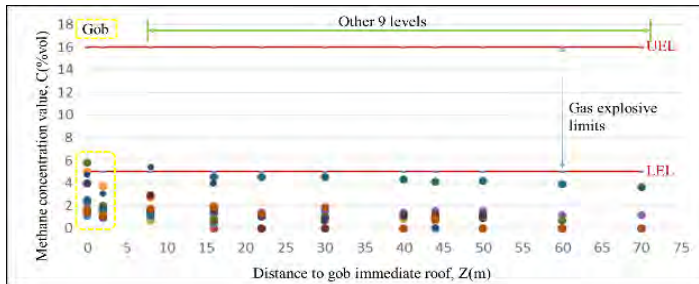
(c)

Figure 14 Scattering diagram of methane concentration values under different methane releasing rate when air quantities in air intake way and return way are separately 2 m/s and 4 m/s (CM 2), (a) GRR = 16.67 m³/min (b) GRR = 33.33 m³/min (c) GRR = 50 m³/min (d) GRR = 66.67 m³/min (continued) (see online version for colours)

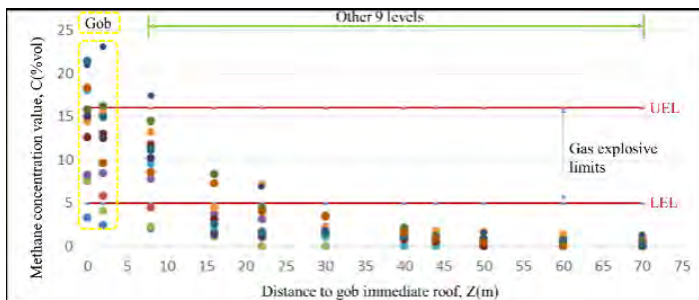


(d)

Figure 15 Scattering diagram of methane concentration values under different methane releasing rate when air quantities in air intake way and return way are separately 2.5 m/s and 3.5 m/s (CM 3), (a) GRR = 16.67 m³/min (b) GRR = 33.33 m³/min (c) GRR = 50 m³/min (d) GRR = 66.67 m³/min (see online version for colours)

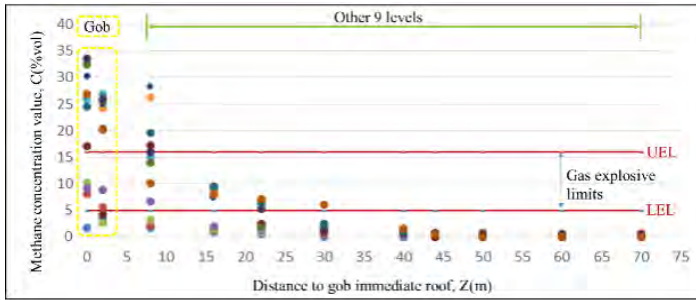


(a)

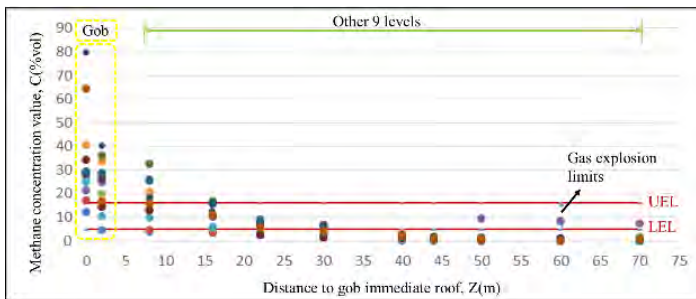


(b)

Figure 15 Scattering diagram of methane concentration values under different methane releasing rate when air quantities in air intake way and return way are separately 2.5 m/s and 3.5 m/s (CM 3) (a) GRR = 16.67 m³/min (b) GRR = 33.33 m³/min (c) GRR = 50 m³/min (d) GRR = 66.67 m³/min (continued) (see online version for colours)



(c)



(d)

The gas concentration pattern in the gob and the overlying strata is very different from the above two cases when air quantities in air intake/return way are set at CM 3. From Figure 14, it must be noted that the gas explosive limits in (b), (c), (d) are narrower than that in (a), because the gas concentration at most measuring points in most levels are very huge which makes Y-axis have to show huger number with a unified length. This explains the shrinkage of gas explosive limits which represent the same range as in other figures. From Figure 15(b), when GRR is set as 33.33 m³/min, about 75% of the area of 8 m level is explosively hazardous and about 17% of the area of 16 m and 22 m levels are potential for an explosion. When GRR is increased to 50 m³/min and 66.67 m³/min, even part of the area of 30 m level is explosive.

6 Conclusions

A 3D physical model is developed to investigate the gas concentration pattern in the mine gob and overlying strata. In the model, parameters including the physical dimensions for the model frame and variables involved in similarity of gas flow are all well considered

in terms of dimensional analysis, which could make the modelling results more reliable to simulate the actual ventilation features in real mine gobs.

The gas flow simulation experiments in the physical model indicate that the gas concentration in the gob area and overlying strata is mostly influenced by the ventilation modes and GRRs and it varies from the levels with different height. According to the experimental results, the gas concentration on upper level is significantly greater than that on lower level in the gob, and the gas explosive zones in overlying strata are mostly scattered in the area from mining coal seam up to 30 m.

Experimental studies are performed with different combinations of CMs and GRRs to investigate the co-effect of ventilation and gas release to gas concentration in the gob and the overlying strata. Among experimental data, the ventilation mode of CM 3 (2.5 m/s and 3.5 m/s) is an ideal ventilation plan to control the gas in the gob when GRR is over 50 m³/min, because it can mitigate the explosive danger in the gob by eliminating the gas accumulation. The gas concentration can be over UEL when GRR is set as 66.67 m³/min in a certain special period of time. It also reveals that the other several levels in overlying strata possibly have the gas explosion risk, especially the deformed strata close to gob roof, where the gas could accumulate to reach the lower explosion limit and result in an explosion. Hence, the explosion-proof technologies should be implanted instantly once the explosively dangerous area is enlarged from the gob area to the upper space.

Acknowledgements

This work is financially supported by grants from the National Science Foundation of China (Grant No. 51304203 and 51574232), Independent Research Projects of State Key Laboratory of Coal Resources and Safe Mining, CUMT (Grant No. SKLCRSM18X002), Fundamental Research Funds for Central Universities (Grant No. 2015XKMS007), China Post-doctoral Science Foundation Special Financial Grant funded project (Grant No. 2016T90528) and Priority Academic Program Development of Jiangsu Higher Education Institutions; the authors are grateful for these supports.

References

- Airey, E. (1968) 'Gas emission from broken coal. An experimental and theoretical investigation', *International Journal of Rock Mechanics and Mining Sciences & Geomechanics Abstracts*, Vol. 5, No. 6, pp.475–494.
- Balusu, R., Deguchi, G., Holland, R., Moreby, R., Xue, S., Wendt, M. and Mallet, C. (2001) 'Goaf gas flow mechanics and development of gas and Sponcom control strategies at a highly gassy coal mine', Paper presented at the *Australia-Japan Technology Exchange Workshop*, Hunter Valley, Australia, 3–4 December 2001.
- Chen, H., Qi, H., Long, R. and Zhang, M. (2012) 'Research on 10-year tendency of China coal mine accidents and the characteristics of human factors', *Safety Science*, Vol. 50, No. 4, pp.745–750.
- Cheng, J., Li, S., Zhang, F., Zhao, C., Yang, S. and Ghosh, A. (2016) 'CFD modelling of ventilation optimization for improving mine safety in longwall working faces', *Journal of Loss Prevention in the Process Industries*, Vol. 40, No. 3, pp.285–297.
- Choi, S.K., Wold, M. and Wood, J. (1997) 'Modelling of interburden gas flows at appin colliery', Paper presented at the *Symposium on Safety in Mines: the Role of Geology*, Newcastle, Australia, 11–12 November 1997.

- Curl, S. (1978) *Methane Prediction in Coal Mines*, IEA Coal Resources Report ICTIS/TR 04.
- Diamond, W., Jeran, W. and Trevits, M. (1994) *Evaluation of Alternative Placement of Longwall Gob Gas Ventholes for Optimum Performance*, US Department of the Interior, Bureau of Mines, RI 9500.
- Dougherty, H., Karacan, C. and Goodman, G. (2010) 'Reservoir diagnosis of longwall gobs through drawdown tests and decline curve analyses of gob gas venthole productions', *International Journal of Rock Mechanics and Mining Sciences*, Vol. 47, No. 5, pp.851–857.
- Flores, R.M. (1998) 'Coalbed methane: from hazard to resource', *International Journal of Coal Geology*, Vol. 35, Nos. 1–4, pp.3–26.
- Hu, G., Wang, H., Fan, X., Yuan, Z. and Hong, S. (2009) 'Mathematical model of coalbed gas flow with Klinkenberg effects in multi-physical fields and its analytic solution', *Transport in Porous Media*, Vol. 76, No. 3, pp.407–420.
- Hu, G., Wang, H., Tan, T., Fan, X. and Yuan, Z. (2008) 'Gas seepage equation of deep mined coal seams and its application', *Journal of China University of Mining and Technology*, Vol. 18, No. 4, pp.483–487.
- Jones, R. (1969) 'Blood flow', *Annual Review of Fluid Mechanics*, Vol. 1, No. 1, pp.223–244.
- Karacan, C.O. (2015) 'Analysis of gob gas venthole production performances for strata gas control in longwall mining', *International Journal of Rock Mechanics and Mining Sciences*, Vol. 79, No. 10, pp.9–18.
- Karacan, C.O., Esterhuizen, G.S., Schatzel, S.J. and Diamond, W. (2007) 'Reservoir simulation-based modeling for characterizing longwall methane emissions and gob gas venthole production', *International Journal of Coal Geology*, Vol. 71, Nos. 2–3, pp.225–245.
- Karacan, C.O., Ruiz, F., Cote, A. and Phipps, S. (2011) 'Coal mine methane: a review of capture and utilization practices with benefits to mining safety and to greenhouse gas reduction', *International Journal of Coal Geology*, Vol. 86, Nos. 2–3, pp.121–156.
- Konduri, I., McPherson, M. and Topuz, E. (1997) 'Experimental and numerical modeling of jet fans for auxiliary ventilation in mines', Paper presented at the *6th International Mine Ventilation Congress*, Pittsburgh, USA, 17–22 May 2006.
- Kundu, P. and Cohen, I. (2008) *Fluid Mechanics*, 4th ed., Elsevier, Burlington.
- Liu, Y., Shao, S., Wang, X., Chang, L., Cui, G. and Zhou, F. (2016) 'Gas flow analysis for the impact of gob gas ventholes on coalbed methane drainage from a longwall gob', *Journal of Natural Gas Science and Engineering*, Vol. 36, Part B, pp.1312–1325.
- Lunarzewski, L. (1998) 'Gas emission prediction and recovery in underground coal mines', *International Journal of Coal Geology*, Vol. 35, Nos. 1–4, pp.117–145.
- Mishra, D., Kumar, P. and Panigrahi, D. (2016) 'Dispersion of methane in tailgate of a retreating longwall mine: a computational fluid dynamics study', *Environmental Earth Sciences*, Vol. 75, No. 6, pp.1–10.
- Palchik, V. (2003) 'Formation of fractured zones in overburden due to longwall mining', *Environmental Geology*, Vol. 44, No. 1, pp.28–38.
- Prosser, B. and Oswald, N. (2006) 'Ventilation surveying and modeling of longwall bleeder and gob areas', Paper presented at the *11th US/North American Mine Ventilation Symposium*, University Park, USA, 5–7 June 2006.
- Schatzel, S., Garcia, F. and McCall, F. (1992) 'Methane sources and emissions on two longwall panels of a Virginia coal mine', Paper presented at the *9th Annual International Pittsburgh Coal Conference*, Pittsburgh, USA, 28–29 October 1992.
- Schatzel, S.C., Karacan, O., Dougherty, H. and Goodman, G. (2012) 'An analysis of reservoir conditions and responses in longwall panel overburden during mining and its effect on gob gas well performance', *Engineering Geology*, Vol. 127, pp.65–74.
- Singh, M. and Kendorski, F. (1981) 'Strata disturbance prediction for mining beneath surface water and waste impoundments', Paper presented at the *1st Conference on Ground Control in Mining*, Morgantown, USA, 27–29 July 1981.

- Stoltz, R., Francart, W., Adair, L. and Lewis, J. (2006) 'Sealing a recent United States coal mine longwall gob fire', Paper presented at the *11th US/North American Mine Ventilation Symposium*, University Park, USA, 5–7 June 2006.
- Torano, J., Tomo, S., Menendez, M., Gent, M. and Velasco, J. (2009) 'Models of methane behaviour in auxiliary ventilation of underground coal mining', *International Journal of Coal Geology*, Vol. 80, No. 1, pp.35–43.
- Wallerstein, N., Alonso, C., Bennett, S. and Thorne, C. (2002) 'Surface wave forces acting on submerged logs', *Journal of Hydraulic Engineering*, Vol. 128, No. 3, pp.349–353.
- Wang, L., Wu, F., Tian, D., Li, W., Fang, L., Kong, C. and Zhou, M. (2015) 'Effects of Na content on structural and optical properties of Na-doped ZnO thin films prepared by sol-gel method', *Journal of Alloys and Compounds*, Vol. 623, pp.367–373.